Soft Matter

Dynamic Article Links

Cite this: *Soft Matter*, 2011, **7**, 11259

www.rsc.org/softmatter

PAPER

Thermosensitive nanogels based on dendritic polyglycerol and N-isopropylacrylamide for biomedical applications†

Julio C. Cuggino,[a] Cecilia I. Alvarez I,[a] Miriam C. Strumia,[a] Pia Welker,[b] Kai Licha,[b] Dirk Steinhilber,[c] Radu-Cristian Mutihac[c] and Marcelo Calderón*[c]

Received 19th July 2011, Accepted 23rd September 2011
DOI: 10.1039/c1sm06357j

In this paper we describe a methodology for the synthesis of thermoresponsive polyglycerol-based nanogels through precipitation polymerization. A systematic analysis of the preparative conditions and composition regarding the nanogel size is presented. The thermoresponsive properties of the synthesized nanogels, as well as the cytotoxicity and uptake in three different cell lines were investigated. The thermoresponsive behavior, the enhanced biocompatible profile, and the cell penetrating properties of the nanogels highlight the potential of such constructs for application as smart, environmentally-responsive materials.

Introduction

The effort to design and develop materials on the nanometre scale has been accelerating at a fast pace in recent decades. In the field of biomedicine, stimuli-responsive and biocompatible materials have emerged as the new generation of smart molecules/materials. In general, the operating principle behind responsive architectures lies in the fact that different environmental triggers can lead to structural/chemical changes within the scaffold of such materials. This unique feature enables their use in diversified biomedical applications.[1,2] The development of sensitive molecular nanostructures with well-defined particle architecture is of interest in biomedical applications as drug delivery, pH-sensors, and imaging agents.[3]

In an attempt to create very well-defined, monodisperse, stable nanostructures at the molecular level, highly branched dendritic polymers have been used for last couple of decades. Special interest has been devoted to the fabrication of nanogels which are high molecular weight cross-linked polymers that combine the characteristics of dendritic polymers with that of cross-linked macroscopic gels, to yield soluble particles within the useful size range between 20 and 350 nm. Our group has developed several methodologies for preparing dendritic polyglycerol (PG)-based nanogels.[4–9] Dendritic PGs, obtained by ring-opening polymerization of glycidol, are usually characterized by tunable end group functionalities, defined topological 3D architecture, and inertness to non-specific interactions with biological systems, are a novel platform for next generation biomaterials.[10]

Stimuli-sensitive nanogels are polymeric macro architectures consisting of a cross-linked, three-dimensional network that can respond to local environmental conditions. They can shrink or swell rapidly by expelling or absorbing water in response to external stimuli such as temperature, pH, electrical, and magnetic fields.[11–19] Thermoresponsive polymers in particular have been shown to have great potential in several fields. Poly(*N*-isopropylacrylamide) (PNIPAm) has been the gold standard for temperature-sensitive applications, because aqueous solution of PNIPAm and its copolymers undergo a reversible phase-transition temperature close to the physiological temperature (32–33 °C).[20–25] The use of PNIPAm in the biomedical field, however, has been limited due to its lack of water solubility above the lower critical solution temperature (LCST), its non-specific protein absorption, and its poor biocompatibility profile.

Several publications have reported the potential of dendritic polyglycerol scaffolds with thermoresponsive properties and diameters lower than 10 nm.[26–33] However, the potential of such architectures within the size range of 50 and 200 nm still remained unexplored. We present here for the first time a methodology for synthesis of thermoresponsive polyglycerol-based nanogels combining the biocompatibility, high functionality, antifouling properties,[34–38] and water solubility of PG with particular sizes ranging from 50 to 200 nm. Precipitation polymerization was used as a convenient synthetic methodology to yield thermosensitive nanogels based on PNIPAm and hyperbranched polyglycerol (HPG). HPG was incorporated to enhance the water solubility and biocompatibility of the nanogels

[a]*IMBIV-CONICET, Departamento de Química Orgánica, Facultad de Ciencias Químicas, Universidad Nacional de Córdoba, Haya de la Torre y Medina Allende, Edificio de Ciencias II, Ciudad Universitaria, Córdoba, Argentina*
[b]*mivenion GmbH, Robert-Koch-Platz 4, Berlin, 10115, Germany*
[c]*Institut für Chemie und Biochemie, Freie Universität Berlin, Takustrasse 3, Berlin, 14195, Germany. E-mail: calderonmarcelo@yahoo.es; Web: http://www.polytree.de; Fax: (+49) 30-838-53357*

† Electronic Supplementary Information (ESI) available: nanogel characterization, thermoresponsive reversibility, TEM, interference enhanced reflection light microscopy video, cytotoxic assay results, and cellular uptake analysis. See DOI: 10.1039/c1sm06357j/

as well as to tune the thermoresponsive profile as a function of the nanogel size in the solution. A systematic analysis of the preparative conditions and composition regarding the nanogel size has been performed. The thermoresponsive behavior, the enhanced biocompatible profile, and the cell penetrating properties of the nanogels highlight the potential of such constructs for application as smart, environmentally-responsive materials.

Experimental

Materials

The following chemicals were used as purchased: acryloyl chloride (AC, 96% Fluka), triethylamine (TEA, 99% Acros), dry dimethylformamide (DMF, 99.8% Acros), N-isopropylacrylamide (NIPAm, 97% Aldrich), poly(ethylene glycol) dimethacrylate (PEGDMA Mn 258 g mol^{-1}, Aldrich), ammonium persulphate (APS, 98% Aldrich), sodium dodecyl sulphate (SDS, 98% Across), tetramethylenethylendiamine (TEMED, 99% Aldrich), rhodamin B hydrochloride (ROD B, 95% Aldrich), *N*,*N*′-dicyclohexylcarbodiimide (DCC, 99% Aldrich), 4-(dimethylamino)pyridine (DMAP, 99% Aldrich).

Synthesis of 5% acrylated hyperbranched polyglycerol (5% Ac-HPG)

Hyperbranched PG with average Mw of 10 kDa was synthesized according to previously reported methodologies.[39] For the synthesis of the acrylated HPG derivative a cold solution of acryloyl chloride (0.11 mL, 1.35 mmol) in dry DMF (4 mL) was added dropwise to a stirred solution of HPG (2 g, 10 kDa, 27.03 mmol OH equivalent) and TEA (0.24 mL, 1.72 mmol) in DMF (60 mL) at 0 °C. The reaction was then allowed to run at 25 °C for 4 h. After the reaction, the solvent was concentrated by cryo-distillation and 50 mL of water was added to the condensate. The acrylated HPG at 5% level of OH groups functionalization (5% Ac-HPG) was purified by dialysis in water for 2 days and then stored in solution with stabilizer (p-methoxy phenol) at 4 °C. ^{1}H-NMR (500 MHz, D_2O), δ: 3.0–4.6 (m, 5H), 5.76–5.90 (m, 1H), 6.02–6.18 (m, 1H), 6.30–6.48 (m, 1H). IR (cm^{-1}): 3100–3500 (OH, HPG), 1636 (CO amide NIPAm), 1536 (amide NIPAm), 1386 (CH isopropyl group NIPAm), 1366 (CH isopropyl group NIPAm), 1070 (C–O, HPG) (see S2 in Supporting Information for details - SI).

Synthesis of nanogels

In a typical procedure for the synthesis of the nanogels, a certain amount of NIPAm, 5% Ac-HPG, SDS, and APS was dissolved in distilled water in a flask and stirred for 15 min under argon atmosphere. Then, the mixture was transferred to a hot bath at 68 °C and the polymerization process was activated after 5 min with the addition of a catalytic amount of a TEMED solution (0.32 M). The mixture was stirred at 250 rpm at 68 °C under argon for 4 h. The product was dialyzed for 2 days in water using dialysis membrane (MWCO 25000) and then lyophilized to obtain a white solid with yields between 80% and 90%. Nanogels with different sizes were prepared by a systematic variation of the NIPAm/HPG feed-ratio and concentration, as well as the surfactant composition. In detail, all the reaction were performed using 100 mg of NIPAm (except 33% HPG-A with 75 mg of NIPAm), 1.8 mg of SDS (except 33% HPG-C with 2.8 mg SDS), 2.8 mg of APS, and 120 μL of TEMED (0.32 M) as activator in 5 mL of distilled water. A PNIPAm nanogel without HPG (0% HPG, Table 1) was prepared as control. For the preparation of 0% of HPG, PEGDMA was used as cross-linking agent in order to replace the cross-linking function of 5% Ac-HPG.

Chemical structure characterization

^{1}H-NMR analysis was performed using a Bruker 500 MHz NMR spectrometer. The sample preparation, in which 8 mg of nanogel had been dissolved in 0.8 mL of D_2O, was performed 24 h prior to the measurement. FT-IR analysis was carried out using a Bruker IFS 66 FT-IR spectrophotometer in the range of 4000–500 cm^{-1}.

Dynamic light scattering (DLS) and zeta potential

The nanogel particle sizes and the dispersity were measured at various temperatures ranging from 22 to 45 °C by dynamic light scattering using a Nano-ZS 90 Malvern equipped with a He–Ne laser ($\lambda = 633$ nm) under scattering of 173°. All the samples were maintained for stabilization at the designed temperature for 5 min before testing. The samples were prepared dissolving 1 mg of dry nanogel in 1 mL of buffer phosphate pH = 7.4 one day prior to the experiments. Particle sizes and size distribution are given as the average of 3 measurements from the volume distribution curves.

Transmission electron microscopy (TEM)

Transmission electron microscopy samples were prepared on copper grids (200 meshes) by blotting samples in 1% aqueous phosphotungstic acid and visualized using a Philips CM12 Electron Microscope. 1 mg of each nanogel was dissolved in 1 mL of deionized water one day before the TEM experiment. Prior to the blotting process, the nanogel solutions were equilibrated in a bath at 26 or 37 °C for 10 min; rapidly a drop of each nanogels solution was added on the copper grids surface, followed by a drop of phosphotungstic acid. The excess of water was evaporated in an oven at 30 °C for 2 min.

Atomic force microscopy (AFM)

The AFM tapping mode images were recorded in the air under ambient conditions, with a MultiMode 8 AFM equipped with a Nanoscope V controller from Veeco Instruments, Santa Barbara, California. The results were analyzed by means of NanoScope Analysis 1.3 software. The nanogels were spread on pieces of silicon wafers ($\approx$ 1 cm × 1 cm) *via* spin-coating from aqueous solution (ambient conditions, room temperature). The wafers (Si-100, p (boron), 30 ohm cm) were obtained from Silchem, Freiberg, Germany. They had artificially oxidized surfaces (wet oxidation) with an oxide layer thickness of about 300 nm. Before the spin coating procedure, the wafers were treated with a piranha solution (3 : 1 mixture of sulphuric acid and 30% hydrogen peroxide) in order to eliminate any organic impurities from the surface.

Table 1 Properties of the thermoresponsive nanogels

Product	Nanogel diameter (nm)[a] 26 °C	Nanogel diameter (nm)[a] 37 °C	Size decrease (%)	CP (°C)[b]
0% HPG[c]	220	[d]	—	32.5
22% HPG	158	83	47	33.0
33% HPG-A	78	62	20	33.3
33% HPG-B	137	72	47	33.1
33% HPG-C	101	60	41	33.4
50% HPG	95	60	36	34.6
60% HPG	75	58	23	34.4

[a] Obtained from the size distribution by volume *via* DLS measurements. [b] Measured by turbidimetry. [c] Nanogel prepared without HPG; PEGDMA was used as cross-linking agent. [d] Precipitation was observed.

Interference enhanced reflection light microscopy

The thermoresponsive behavior of the nanogels was visualized online with an interference enhanced optical reflection microscopy tuned with a heating/cooling stage.[40] This technique along with an optimized combination of the oxide layer thickness (typically 300 nm) and wavelength led to an intensity contrast high enough to visualize features on the surface in the range of nanometres.[41] Several temperature cycles were run between 20 °C and 40 °C in the air under ambient conditions in order to check the reproducibility of the results. The temperature controller allowed an exact control of the temperature in a range of 0.1 °C with a heating/cooling rate between 0.1 °C and 20 °C per minute. The data for the analysis was collected by changing the temperature stepwise and allowing at each recorded point sufficient time for the system to stabilize and reach equilibrium. The results depicted are the average value between the heating and cooling processes, and are expressed as an average of three consecutive cycles. For further image optimization, data were digitally processed by running ImageJ software.

Cloud point determination by UV-Visible measurement

Cloud points were measured on a Cary 100 Bio UV-Vis spectrophotometer equipped with a temperature-controlled, six-position sample holder. Buffer phosphate pH 7.4 nanogels solutions (1 mg mL^{-1}) were heated at 0.2 °C min^{-1} while monitoring both the transmittance at 500 nm (1 cm path length) and the solution temperature (from 22 to 45 °C), as determined by the internal temperature probe. The cloud point (CP) of each nanogel was determined using the minimum of the first derivate of graph %T *vs.* temperature.

Cellular analysis

Rhodamin B labelling of nanogels. In a typical procedure 0.5 mg of ROD B, 0.4 mg of DCC, and 0.01 mg of DMAP were dissolved in 0.8 mL of dry DMF under stirring at 0 °C for 10 min. Subsequently, 4 mg of nanogel dissolved in 0.2 mL dry DMF was added. The mixture was stirred overnight and then purified using a sephadex column (G-25 superfine) eluted with water. The polymer attached at ROD B was then dialyzed for 2 days in deionized water and lyophilized to yield the polymer-dye conjugate.

Cell culture. The human lung cancer A549 cell line and the human epidermoid cell line A431 were routinely cultured in DMEM medium, with 10% fetal calf serum (FCS), 2% glutamine, and penicillin/streptomycin (all from PAN Biotech) added. All cells were seeded into medium at 1×10^5 cells mL^{-1}, cultured at 37 °C with 5% CO_2, and split 1 : 5 two times a week. The human hematopoietic cell line U-937 was routinely propagated as follows: RPMI medium (PAN Biotech), with 10% fetal calf serum (FCS) and penicillin/streptomycin. Cells were seeded into medium at 1×10^5 cells mL^{-1}, cultured at 37 °C with 5% CO_2, and split 1 : 30 two times a week.

Cytochemical staining. In the present study, cell were seeded at 2×10^5 cells mL^{-1} in a 24-well culture plate on glass coverslips (Sigma), and cultured for 24 h at 37 °C. Thereafter, cells were incubated with medium alone or containing 0.5 mg mL^{-1} solution of ROD B labelled nanogels for 4 h at 37 °C. Afterwards, cells were fixed with cold acetone, rinsed, and covered with Alexa Fluor 488 Phalloidin (1 : 300, Molecular Probes) for staining of actin cytoskeleton. Image acquisition was performed using a Leica DMRB microscope (Leica).

Cytotoxicity assays. These analyses were performed with U937 cells cultured in 24-well-plates. 2×10^5 cells mL^{-1} were incubated in 1 mL culture medium containing increasing concentration of rhodamin B labelled nanogels (n = 4). After two days of culture, drug cytotoxicity was assessed *in vitro* using the MTT assay (cellular reduction of 3-(4,5-dimethylthiazol-2-yl)-2,5-diphenyltetrazolium bromide) as a test for metabolic activity of the cells. Briefly, 1×10^4 cells per well were plated in 96-well plates in 100 μL culture medium containing increasing concentration of the test substance in quadruplicate. 10 μL MTT (5 mg mL^{-1} in PBS, obtained from Millipore) was added to each well and the plates were incubated for 4 h. The resulting formazan product was dissolved with acid isopropanol and the absorbance at a wavelength of 570 nm (Ex570) was read on a Microplate Spectrophotometer (Anthos htII, Microsystems). In addition, cell number and viability was detected in a CASY analyser (Schärfe systems).

Results and discussion

Synthesis of nanogels

There has always been a great need for new methodologies which allow preparation of soft materials with controllable size and low variation of particle size. In this context we undertook the

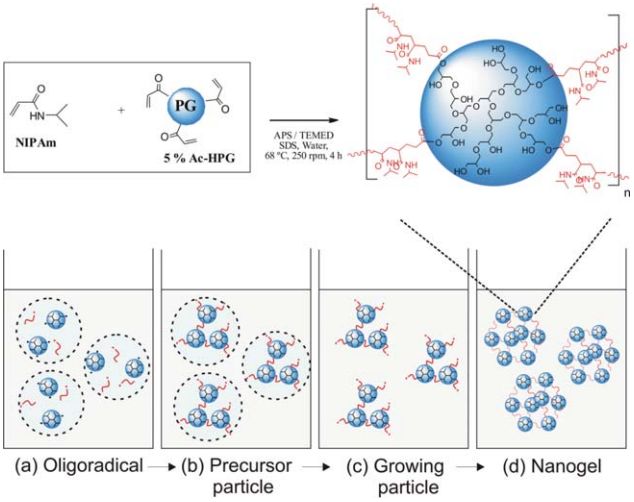

Fig. 1 Synthesis of the nanogels using precipitation polymerization with NIPAm as monomer, partially acrylated HPG with MW 10 kDa as macrocross-linker (5% Ac-HPG), SDS as surfactant for oligoradical stabilization, APS/TEMED as redox radical initiator, and deionized water as solvent.

challenge of applying precipitation polymerization to synthesize thermoresponsive nanogels based on PG with readily available building blocks as starting materials. Generally, in the precipitation polymerization the growing monomer chains are kept together in a living network which after reaching a critical length collapses onto itself (a–c in Fig. 1). The precursor particles resulting from the precipitation can grow by addition of the monomer on the precursor particle, by aggregation with the other precursor particles, or by being captured by existing colloidal stable particles.[42,43] In our case, the polyglycerol nanogels are allowed to form by nucleation events that have been triggered by a radical initiation with partially acrylated HPG as cross-linking points and PNIPAm as growing chains that have been stabilized by sodium dodecyl sulphate (SDS) below the critical micelle concentration (CMC) at 68 °C (above the LCST of PNIPAm). This facile method was found to be extremely versatile for the synthesis of nanoparticles with a narrow size distribution and a high particle size control. Fig. 1 shows the schematic synthesis of nanogels using NIPAm as monomer, partially acrylated HPG with MW 10 kDa as macrocross-linker (5% Ac-HPG), SDS as surfactant, APS/TEMED as redox radical initiator, and deionized water as solvent. As a key to control the precipitation of the precursor particles, the temperature of the reaction mixture was kept above the LCST of PNIPAm. As an initial evaluation of the reaction performance, a systematic analysis was undertaken modifying the NIPAm/HPG feed-ratio and concentration, as well as the surfactant composition. Several water soluble and well-defined spherical nanogels were obtained by this process with different sizes (ranging from 60 to 158 nm) and polyglycerol compositions between 20% and 60% w/w. This method yielded nanogel particles in the nanometre range with narrow size distribution, as demonstrated by dynamic light scattering (particles with dispersity lower than 0.1 at 37 °C—see Table S1 in ESI†) and transmission electron microscopy (TEM). All the nanogels had conversions of above 80% while preserving the initial feed ratio between NIPAm and HPG as confirmed by ^{1}H-NMR and FT-IR (see Fig. S3 in ESI†).

Characterization

Dynamic light scattering measurements allowed determination of the hydrodynamic diameter from the polyglycerol-based nanogels. Table 1 shows the size of the HPG-*co*-PNIPAm nanogels in buffer phosphate pH 7.4 at 26 °C or 37 °C measured by DLS. As can be seen in Table 1 (first column), the size of the nanogels could be tuned by modifying the HPG composition and the monomers or surfactant concentration. As expected, at 26 °C an increment on the percentage of HPG in the structure (22% HPG, 33% HPG-B, 50% HPG, and 60% HPG) resulted in a decrease of diameter of the nanogels from 158 nm to 75 nm due to the higher amount of cross-linking points in the network. In addition, the size of the nanogels using an equal percentage of HPG probed to be tuneable to a smaller size by decreasing the concentration of monomers (33% HPG-A) or increasing the amount of the surfactant (33% HPG-C) as already shown by Blackburn *et al.*[44] Additionally, the nanogel without HPG in the structure (with PEGDMA as cross-linker) showed a diameter of 220 nm at this temperature. All the nanogels containing HPG in their network were soluble in water in a broad range of temperatures in comparison to the PNIPAm nanogel (HPG 0%), which was found to be water insoluble above its LCST.

The morphology of the nanogels was analyzed by transmission electron microscopy (TEM, Fig. 2a,b) and atomic force microscopy (AFM, Fig. 2c,d). Both techniques demonstrate a well-defined spherical morphology of the dried nanogels onto a copper or silica surface.

Thermoresponsive properties

The aqueous solutions containing nanogel were analyzed according to the particle size and the UV-Vis transmittance within a range of temperature from 22 to 45 °C. Measurements of transmittance of UV-Vis light from aqueous solutions of nanogels were performed to determine the cloud points (CP) as an

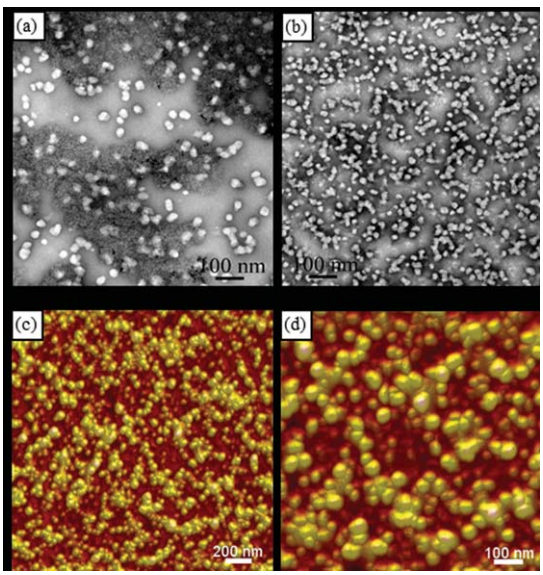

Fig. 2 TEM images of 1 mg mL^{-1} solution in water of 33% HPG-B nanogel blotted at (a) 26 and (b) 37 °C. AFM images of 2 mg mL^{-1} aqueous solution with height images (c) 2.0 μm × 2.0 μm, (d) 1 μm × 1 μm.

indication of thermoresponsive behavior. Transmittance of a heating and a cooling cycle of each nanogel in phosphate buffer pH 7.4 (1 mg mL^{-1}) was measured between 22 to 45 °C at 500 nm using a UV-Vis spectrophotometer equipped with a temperature-control device. A representative heating-cooling cycle for the nanogels 0% HPG and 33% HPG-B is shown in Fig. 3a. The CP detailed in Table 1 corresponded to the minimum point of the first derivate of a %T *vs.* temperature curve and were in the range 32.5–34.6 °C. As expected, with respect to the PNIPAm nanogel (0% HPG), a small increase in the LCST was evident with the incorporation of HPG due to the hydrophilic properties imparted by the polymer. Interesting enough, the thermosensitive properties of the PNIPAm nanogels were stored after the incorporation of up to 60% w/w of HPG in the structure. However, a decrease in the thermoresponsive property with the increase of the HPG content was observed.

The correlation between the nanogel size in solution and the temperature was determined by DLS measurements. Fig. 3b shows the tendency of the nanogels to shrink with an increasing of temperature of the solution. There was a sharp decrease in the nanogel size in temperatures near the CP that demonstrate the shrinkage of nanogel particles driven by enhanced of hydrophobic interaction between the NIPAm fragments above their LCST. The nanogels with HPG in its structure did not precipitate at temperatures above the CP due to substantial hydrophilicity imparted by the polyglycerol counterpart. DLS measurements demonstrated that, unlike other thermoresponsive polymers, the HPG-*co*-PNIPAm nanogels did not aggregate. This is a unique feature so far as the biomedical application of such materials is concerned. The thermoresponsivity of the nanogel was found to be reversible at least for 3 temperature cycles between 26 °C to 37 °C and the time of responsiveness was shorter than two minutes (see Fig. S5 in ESI†).

On the other hand, the thermoresponsive properties of the nanogels blotted on the surfaces of copper (Cu) and SiO_2 were respectively analyzed by TEM and interference enhanced reflection light microscopy. The TEM images depicted in Fig. 2a–b are evidence that the sizes of the nanogels were influenced by the temperature in which the samples were incubated prior to their blotting it in the Cu surface, and that they showed the same tendency to shrink at higher temperature as observed with DLS. The TEM micrographs show a visibly different size between the samples incubated at 26 °C (Fig. 2a) and 37 °C (Fig. 2b). In addition, as the % of HPG decreased in the nanogel structure, *i.e.* decreased cross-linker composition, the nanogels were able to flatten more in the Cu surface and thus appeared larger in the TEM images (see Fig. S6 in ESI† for comparison with 50% HPG).

By interference enhanced reflection light microscopy it was possible to evaluate the thermoresponsive properties of the nanogels in contact with a silica surface in a dynamic fashion. Imaging at different temperatures (Fig. 4a–b for 33% HPG-B and Fig. 4c–d for 60% HPG) revealed that the area covered by the nanogels decreased gradually with increasing temperatures. Upon cooling, the surface occupied by the nanogels showed to grow again (refer to video S7 in ESI†), demonstrating that each temperature leads to specific size of the nanogel in contact with the SiO_2 surface. The difference observed in the domain size was

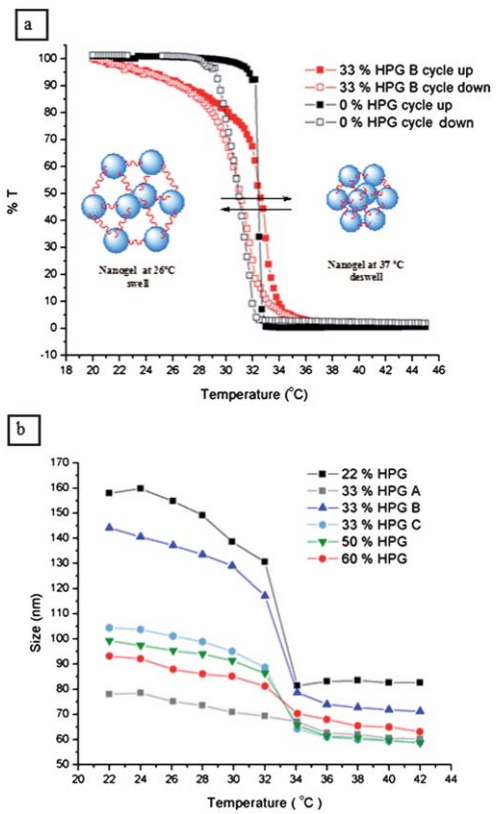

Fig. 3 (a) Transmittance curves of heating/cooling cycle for a 1 mg mL^{-1} of phosphate buffer solution of 0% HPG and 33% HPG-B nanogels. (b) Diameter determined by DLS of 1 mg mL^{-1} solutions of nanogels at different temperatures in buffer phosphate pH 7.4.

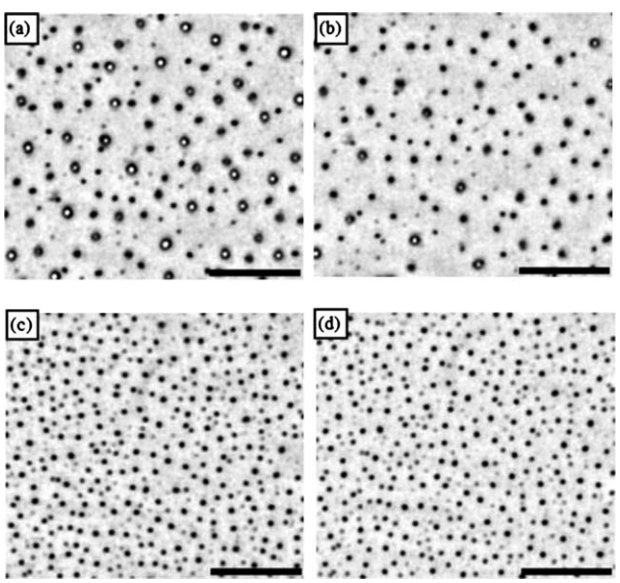

Fig. 4 Interference enhanced reflection light microscopy images on a silica surface. (a,b) 33% HPG-B measured at 20 and 40 °C respectively. (c,d) 60% HPG measured at 20 and 40 °C respectively. Scale bar represents 10 μm in each panel.

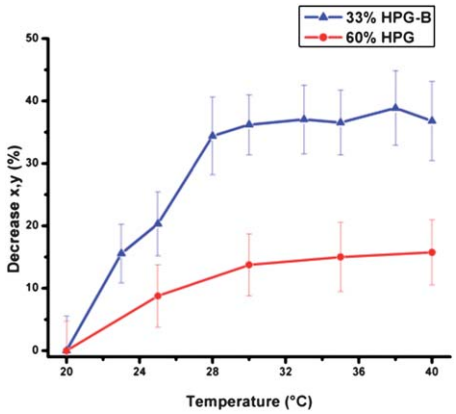

Fig. 5 Size decrease on x,y axes upon heating the sample on a silica surface. The values are expressed as an average of three heating/cooling cycles.

due to changes in the hydrated state of the nanogels which were able to release the adsorbed water molecules from their structure upon an increase in temperature. A movie with the changes induced in the thermoresponsive 33% HPG-B by a continuous increase/decrease of temperature between 20 °C and 40 °C, at a rate of 20 °C per minute, is presented in the ESI (S7). In the images corresponding to 20 °C it can be easily observed that the 33% HPG-B (Fig. 4a) presented larger features on SiO_2 surface than with the 60% HPG (Fig. 4d), following the same tendency described above by DLS.

The results obtained as an average of three heating/cooling cycles for 33% HPG-B and 60% HPG are summarized in Fig. 5 in a representation of the lateral decrease of the nanogels on the surface with the temperature. The graph quantifies the decrease in the surface covered by the nanogels in the SiO_2 surface and confirms the higher thermoresponsive profile from the nanogels with 33% of HPG in the structure.

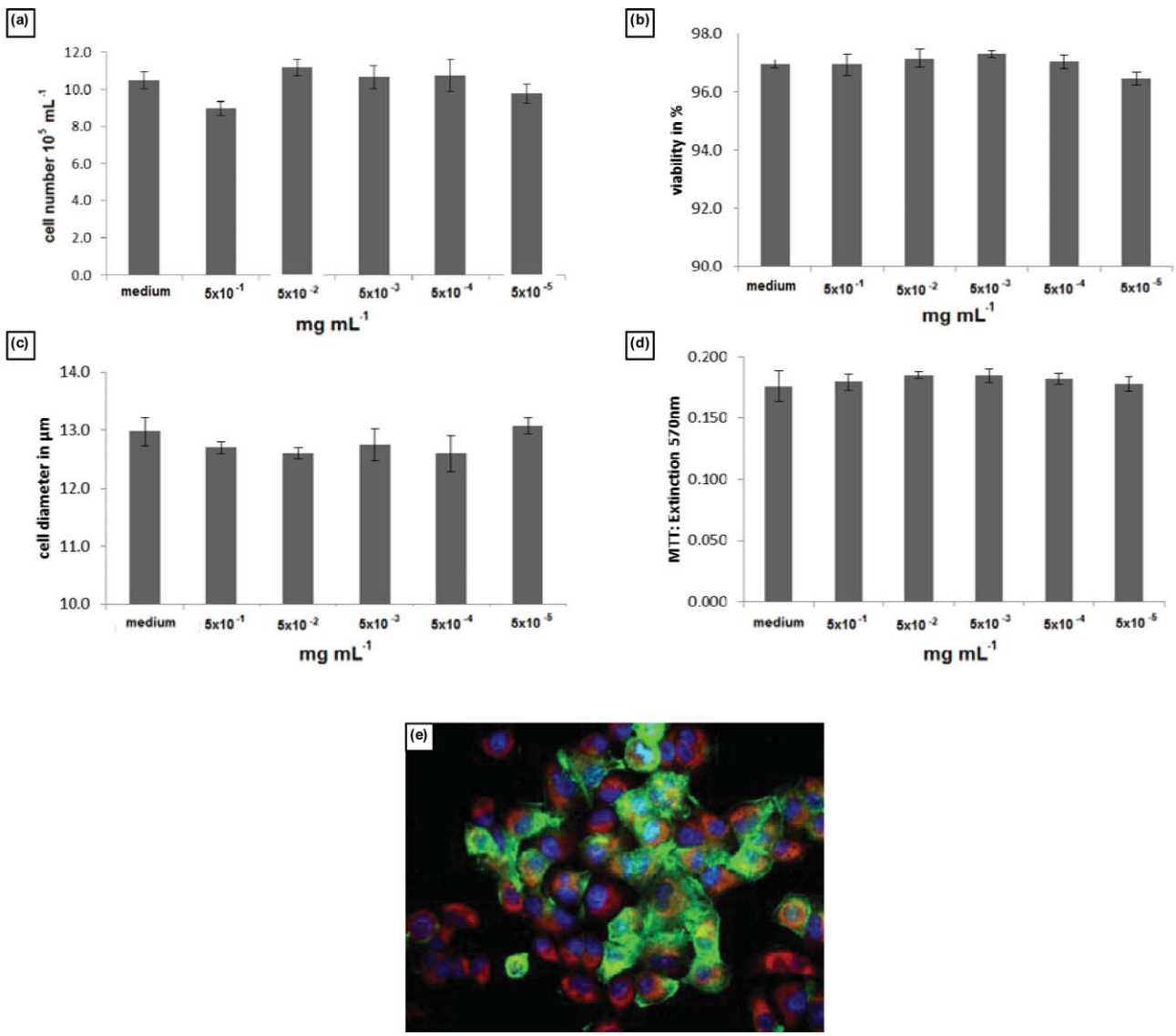

Fig. 6 (a–d) Human hematopoietic U-937 cell proliferation (cell number), viability, cell diameter, and metabolic activity (MTT) tests in a culture with medium or different concentrations of 33% HPG-B nanogel. (e) Typical fluorescence images of A549 lung cancer cells incubated 37 °C with rhodamin B labelled 33% HPG-B nanogel (red). Cytoskeleton was stained with Phalloidin-Alexa488 (green) and the cell nuclei with DAPI (blue). Magnification 1 : 400.

Thermoresponsive nanogel interaction with cells

In order to establish the potential for intracellular delivery of the thermoresponsive HPG-*co*-PNIPAm nanogels, a systematic study was performed to analyze the cytotoxicity and extent of the cellular uptake in three different cell lines, epithelial human lung cancer cell line A549, human hematopoietic cells U-937, and human epidermoid carcinoma cells A431. Cancer cells are subject to apoptosis and other phenotypic properties such as proliferation rates, migration capacity, and ability to induce angiogenesis more significantly than normal cells. Therefore they are ideal for mimicking *in vitro* and as *in vivo* studies over to normal cells.[45] Through fluorescence microscopy the polyglycerol-based nanogels were visualized inside the cells with the help of the coupled rhodamin B dye which showed a red fluorescence. Nuclear and cytoskeleton staining, performed with DAPI and phalloidin-Alexa488 respectively, allowed determination of the intracellular distribution.

Cell compatibility of these materials was probed by investigating effects on cell proliferation (cell number), viability, cell diameter, and metabolic activity (MTT test). Concentrations higher than 0.5 mg mL^{-1} of each nanogel were necessary to promote adverse effects as shown in Fig. 6a–d for 33% HPG-B, which is comparable to other non-cytotoxic polyglycerol-based nanogels elsewhere reported.[5,6] In addition, the thermoresponsive nanogels had cell penetrating properties as shown in Fig. 6e for the ROD-B labelled 33% HPG-B nanogel, with a distribution pattern in the perinuclear region. Some localized regions of high fluorescence intensity were observed, which are expected to correspond to endocytotic vesicles.[6] The same pattern was found for all the nanogels in the A549 and A431 cell lines as shown in the ESI† (Fig. S8 and S9).

As suggested, together with its biodegradability, imparted by the ester linkages, and differential cellular uptake, the new thermoresponsive nanogel should be an ideal candidate for the intracellular delivery of bioactives based in smart modalities. These results are comparable to other HPG-based nanogels which strongly suggest that these highly non-cytotoxic thermoresponsive materials exhibit minor interactions with biological structures which enhance their potential in biomedical fields.

Conclusions

Nanogel technology has already established itself as a robust platform for creation of functional materials with optimal size and multifunctionality for different fields of applications. Fabrication of smart and responsive materials based on nanogels however is still an unchartered area of research.

In this publication, we report for the first time the synthesis of thermosensitive nanogels based on NIPAm and hyperbranched PG through precipitation polymerization. This technique proved to be versatile for synthesis of nanogels with size ranges of 50 to 200 nm with a narrow dispersity. The incorporation of HPG as cross-linking agent enhanced the water solubility of the nanogels, improved their biocompatible profile, and allowed a fine tuning of the thermoresponsive profile regarding the size of the nanogels in solutions. However, the decrease in the thermoresponsive property with the increase of the HPG content should be avoided in future studies. As an alternative, HPG with higher molecular weights or lower acryl-functionality should be used.

Moreover, the biodegradability and multifunctionality of the core structure allows post-modification of the scaffold for encapsulation or conjugation of dyes, drugs, enzymes, *etc.*[10,45–51] The potential in transport and triggered release of bioactives agents is currently under investigation.

Acknowledgements

The authors wish to thank FONCyT, CONICET, CICAL, SECyT (Universidad Nacional de Córdoba), and the FU Focus area "Functional Materials at the Nanoscale" for the financial support. Julio C. Cuggino acknowledges receipt of a fellowship from MECyT- DAAD. The authors would like to acknowledge Dr Adam L. Sisson and Prof. Rainer Haag for their inputs and discussions, and Wiebke Fischer for TEM measurements. Furthermore, Dr Pamela Winchester and Dr Mohiuddin A. Quadir are thanked for careful proofreading of this manuscript.

Notes and references

1 M. Calderon, M. A. Quadir, M. Strumia and R. Haag, *Biochimie*, 2010, **92**, 1242.
2 M. A. Stuart, W. T. Huck, J. Genzer, M. Muller, C. Ober, M. Stamm, G. B. Sukhorukov, I. Szleifer, V. V. Tsukruk, M. Urban, F. Winnik, S. Zauscher, I. Luzinov and S. Minko, *Nat. Mater.*, 2010, **9**, 101.
3 W. Wu, J. Shen, P. Banerjee and S. Zhou, *Biomaterials*, 2010, **31**, 8371.
4 A. L. Sisson, I. Papp, K. Landfester and R. Haag, *Macromolecules*, 2009, **42**, 556.
5 A. L. Sisson, D. Steinhilber, T. Rossow, P. Welker, K. Licha and R. Haag, *Angew. Chem., Int. Ed.*, 2009, **48**, 7540.
6 D. Steinhilber, A. L. Sisson, D. Mangoldt, P. Welker, K. Licha and R. Haag, *Adv. Funct. Mater.*, 2010, **20**, 4133.
7 D. Steinhilber, S. Seiffert, J. A. Heyman, F. Paulus, D. A. Weitz and R. Haag, *Biomaterials*, 2011, **32**, 1311.
8 A. L. Sisson and R. Haag, *Soft Matter*, 2010, **6**, 4968.
9 H. Zhou, D. Steinhilber, H. Schlaad, A. L. Sisson and R. Haag, *React. Funct. Polym.*, 2011, **71**, 356.
10 M. Calderon, M. A. Quadir, S. K. Sharma and R. Haag, *Adv. Mater.*, 2010, **22**, 190.
11 S. R. Deka, A. Quarta, R. Di Corato, A. Falqui, L. Manna, R. Cingolani and T. Pellegrino, *Langmuir*, 2010, **26**, 10315.
12 W. H. Blackburn, E. B. Dickerson, M. H. Smith, J. F. McDonald and L. A. Lyon, *Bioconjugate Chem.*, 2009, **20**, 960.
13 W. Wu, T. Zhou, A. Berliner, P. Banerjee and S. Zhou, *Chem. Mater.*, 2010, **22**, 1966.
14 L. Shi, S. Khondee, T. H. Linz and C. Berkland, *Macromolecules*, 2008, **41**, 6546.
15 T. Nakamura, A. Tamura, H. Murotani, M. Oishi, Y. Jinji, K. Matsuishi and Y. Nagasaki, *Nanoscale*, 2010, **2**, 739.
16 K. Raemdonck, J. Demeester and S. De Smedt, *Soft Matter*, 2009, **5**, 707.
17 M. Oishi, T. Nakamura, Y. Jinji, K. Matsuishi and Y. Nagasaki, *J. Mater. Chem.*, 2009, **19**, 5909.
18 W. Wu, J. Shen, P. Banerjee and S. Zhou, *Biomaterials*, 2011, **32**, 598.
19 M. Guo, C. Que, C. Wang, X. Liu, H. Yan and K. Liu, *Biomaterials*, 2011, **32**, 185.
20 T. Tanaka, *Phys. Rev. Lett.*, 1978, **40**, 820.
21 X. Huang and T. L. Lowe, *Biomacromolecules*, 2005, **6**, 2131.
22 Q. Wang, H. Xu, X. Yang and Y. Yang, *Int. J. Pharm.*, 2008, **361**, 189.
23 T. Niidome, A. Shiotani, T. Mori and Y. Katayama, *J. Controlled Release*, 2010, **148**, e65.
24 C. Gota, K. Okabe, T. Funatsu, Y. Harada and S. Uchiyama, *J. Am. Chem. Soc.*, 2009, **131**, 2766.
25 C. Li and S. Liu, *J. Mater. Chem.*, 2010, **20**, 10716.
26 M. Pan, D. Wan and J. Huang, *Chin. J. Chem.*, 2010, **28**, 499.

27 X. Sun, Y. Zhou and D. Yan, *Macromol. Chem. Phys.*, 2010, **211**, 1940.
28 C. Kojima, K. Yoshimura, A. Harada, Y. Sakanishi and K. Kono, *Bioconjugate Chem.*, 2009, **20**, 1054.
29 C. Kojima, K. Yoshimura, A. Harada, Y. Sakanishi and K. Kono, *J. Polym. Sci., Part A: Polym. Chem.*, 2010, **48**, 4047.
30 D. Wan, Q. Fu and J. Huang, *J. Polym. Sci., Part A: Polym. Chem.*, 2005, **43**, 5652.
31 Y. Shen, M. Kuang, Z. Shen, J. Nieberle, H. Duan and H. Frey, *Angew. Chem., Int. Ed.*, 2008, **47**, 2227.
32 S. Luo, X. Hu, Y. Zhang, C. Ling, X. Liu and S. Chen, *Polym. J.*, 2011, **43**, 41.
33 K. Ranganathan, R. Deng, R. K. Kainthan, C. Wu, D. E. Brooks and J. N. Kizhakkedathu, *Macromolecules*, 2008, **41**, 4226.
34 C. Siegers, M. Bisalski and R. Haag, *Chem.–Eur. J.*, 2004, **10**, 2831.
35 M. Wyszogrodzka, M. Weinhart and R. Haag, *Poly Mat Sci Eng*, 2007, **48**, 760.
36 M. Wyszogrodzka and R. Haag, *Langmuir*, 2009, **25**, 5703.
37 M. Wyszogrodzka and R. Haag, *Biomacromolecules*, 2009, **10**, 1043.
38 M. Weinhart, I. Grunwald, M. Wyszogrodska, L. Gaetjen, A. Hartwig and R. Haag, *Chem.–Asian J.*, 2010, **5**, 1992.
39 R. Haag, S. Mecking, and H. Türk, 2004, Deutsche Patenanmeldung DE 10211664 A1.
40 R. Köhler, P. Lazar and H. Riegler, *Appl. Phys. Lett.*, 2006, **89**, 241906.
41 R.-C. Mutihac and H. Riegler, *Langmuir*, 2010, **26**, 6394.
42 N. Singh, 2008, Doctoral Thesis, Georgia Institute of Technology.
43 R. Pelton, *Adv. Colloid Interface Sci.*, 2000, **85**, 1.
44 W. H. Blackburn and L. A. Lyon, *Colloid Polym. Sci.*, 2008, **286**, 563.
45 J. Khandare, A. Mohr, M. Calderon, P. Welker, K. Licha and R. Haag, *Biomaterials*, 2010, **31**, 4268.
46 M. Calderon, R. Graeser, F. Kratz and R. Haag, *Bioorg. Med. Chem. Lett.*, 2009, **14**, 3725.
47 M. Calderon, R. Haag and F. Kratz, *Journal Onkologie*, 2011, **3**, 152.
48 M. Calderón, P. Welker, K. Licha, I. Fichtner, R. Graeser, R. Haag and F. Kratz, *J. Controlled Release*, 2011, **151**, 295.
49 S. Reichert, P. Welker, M. Calderón, J. Khandare, D. Mangoldt, K. Licha, R. K. Kainthan, D. Brooks and R. Haag, *Small*, 2011, **7**, 820.
50 P. Ofek, W. Fischer, M. Calderon, R. Haag and R. Satchi-Fainaro, *FASEB J.*, 2010, **24**, 3122.
51 W. Fischer, M. Calderon, A. Schulz, I. Andreou, M. Weber and R. Haag, *Bioconjugate Chem.*, 2010, **21**, 1744.

